ABSTRACT

Will be written after most text is done

CONTENTS

LIST OF FIGURES

ACRONYMS

PSF point spread function . . . 3
vAPP vector apodizing phase plate . . . 6
APP apodizing phase plate . . . 5
AO adaptive optics . . . 5
HCIPy high-contrast imaging python . . . 11
ADI angular differential imaging . . . 7
FWHM full width half maximum . . . 21

1 INTRODUCTION

A major and successful topic in astronomy has been the discovery and characterization of exoplanets. This interest has sparked great progress in the field of high contrast imaging resulting in new imaging techniques and instruments. Though as of writing 3,949 planets have been confirmed little is known about their formation. Certain is that a so called protoplanetary disk is an important stage in the formation of a planetary system. The disks can be observed best within the visible spectrum and infrared though ALMA has also had success in observing disks in the radio spectrum.

It is however a great challenge to acquire observations of such a disk due to the high contrast with its star and the required angular resolution. To observe with sufficient resolution adaptive optics are used. This negates most of the atmospheric seeing.

Reducing contrast is done with chronograph, an instrument that blocks out the direct light from a star. The classic Lyot chronograph (Figure 1) blocks direct star light using two foci. In the first focus an opaque mask blocks placed where the star is diffuses and absorbs the direct star light. Then between the foci a ring shaped mask blocks most of the now diffused star light. Then at the second focus the image is made as usual.

However a classical chronograph is not sufficient for observing disks. The vector apodizing phase plate (vAPP) [**papervApp**] is a different type of chronograph placed at the pupil of a telescope. The vAPP blocks starlight by modifying the phase of incoming light. This phase change flips the light in a D-shaped region around the star to the other side. Any faint object next to the star in the now dark region becomes detectable. Compared to the classic Lyot chronograph the vAPP reduces the starlight to a greater degree, see Figure 2.

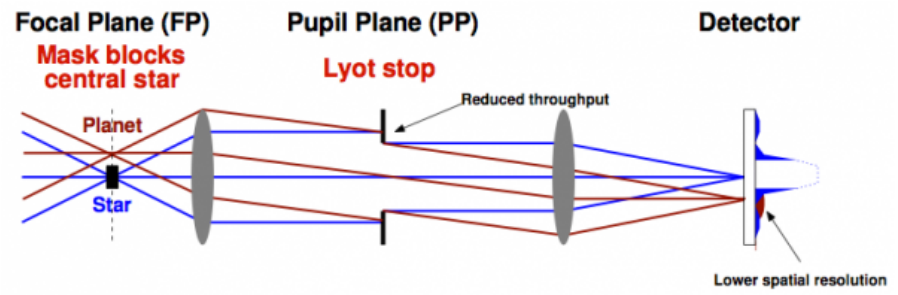

Figure 1: optical layout of a Lyot chronograph, by Matthew Kenworthy, from https://home.strw.leidenuniv.nl/ kenworthy/app

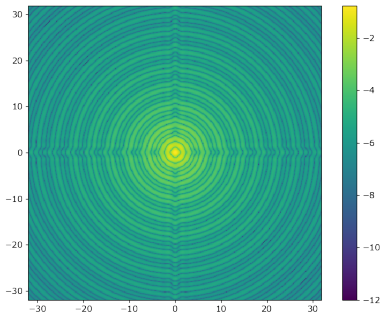

(a) PSF of a classical Lyot chronograph

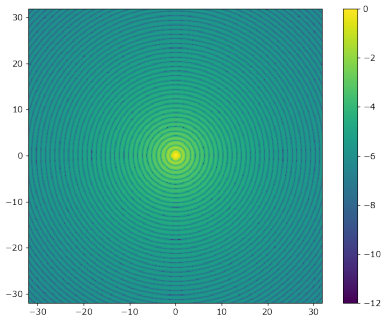

(b) PSF of a telescope without chronograph

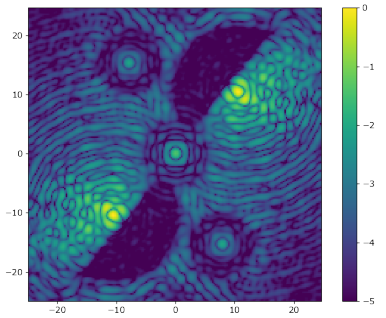

(c) PSF of the vAPP

Figure 2: The PSF is the image an instrument produces when looking at a point source such as a star. Here we sees the PSF of a instrument without a chronograph, with the classical Lyot chronograph and a one using the vAPP

The vAPP has been developed to detect rocky planets in the habitable zone of stars. However it could also allow us to resolve disk features and study disks in greater detail directly. However as the vAPP changes the entire image it is chalking to differentiate disk features from vAPP artifacts.

Here we study what the effect is of both the vAPP and ADI on the apparent morphology of disks.

overview thesis

https://en.wikipedia.org/wiki/Coronagraph

2 THEORY

Here we discuss what an point spread function (PSF) is, how it helps us describe an optical system and how they naturally appear from basic optics. Then we look at the different types of disks that have been observed and what contrasts we expect.

2.1 POINT SPREAD FUNCTION

We can describe what happens to light going through an optical system with its PSF. It describes the light intensity on the focal plane (where the sensor is located) as a function of x and y when a single light ray is imaged on the center of the focal plane.

We derive a way to find the PSF from the Huygens-Fresnel Principle. It states any part of a wave can be described as a front of infinitely many point sources interfering with one another. An optical element can change these arrangement of theses sources, for example an aperture allows only a small area to be filled with these point sources as illustrated in Figure 3.

Figure 3: Fraunhofer diffraction from an arbitrary aperture, r and R large compared to the size of the hole. Extracted from Optics 5th edition, by [4]

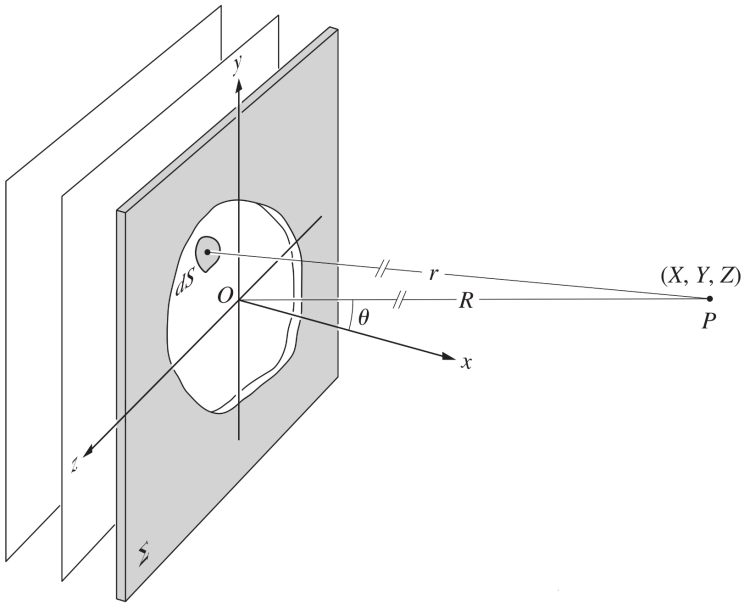

We find the electric field at a point P at distance R by summing up the fields of these infinite point sources taking into account the different distances to R. Writing the infinite sum as an integral we get Equation 1 for the electric field at a point P some distance R from an aperture.

$$E = \frac{\varepsilon_A e^{i(\omega t - kR)}}{R} \iint_{Aperture} e^{ik(Yy+Zz)/R} dS \tag{1a}$$

Here Y, Z describe the position in the imaging plane in which P lies as seen in Figure 3. Small letters y and z are the position in the aperture plane. The integral is over the aperture, only integrating over the transparent parts.

To account for changes in phase and not only magnitude of the field caused by Optical instruments we including an aperture function instead of just integrating over the shape of the aperture. This results in:

$$\mathscr{A}(y,z) = \mathscr{A}_0(y,z)e^{i\phi(y,z)} \tag{2a}$$

Here the amplitude of the aperture function comes from $\mathscr{A}_0$ and the phase from $e^{i\phi(y,z)}$.

$$E(Y,Z) = \iint_{-\infty}^{\infty} \mathscr{A}(y,z)e^{ik(Yy+Zz)/R} dy dz \tag{3a}$$

The expression for the E field at the point P (Equation 1) rewritten to make use of the aperture function.

We can rewrite this to get rid of the dependence on the distance by substituting $K_y = kY/R$ and $K_z = kZ/R$ for Y and Z. This gives the final form:

$$E(K_Y, K_Z) = \iint_{-\infty}^{\infty} \mathscr{A}(y,z)e^{ik(K_Y y+K_Z z)/R} dy dz \tag{4a}$$

This is the 2 dimensional Fourier transformation of the aperture function. Thus "the field distribution in the Fraunhofer diffraction pattern is the Fourier transform of the field distribution across the aperture (e.i., the aperture function)" [4].

For the PSF we are interested in the intensity which is not the electric field E but $|E|^2$. This means we can calculate the PSF of an instrument by Fourier transforming its (complex) aperture function and squaring the result. Note that the amplitude in the aperture function does not only have to depend on the shape of the aperture as there might be partially transparent material. The aperture function does not even have to be an aperture.

With the PSF we know how a single point source would look when imaged by an optical system. If we assume the system is linear system we can use the superposition principle to image extended sources by convolving the PSF with the extended source.

2.1.1 *Atmosphere*

The telescope or chronograph are the only optical system at play. There are many differently moving layers of air between the telescope and space. These work as independent optical systems that change in time. Each layer moves in a different direction at a different speed as winds are different at various altitudes. This changes the phase of the light. The complete PSF changes all the time. The changes are smaller at smaller timescales.

2.1.2 *Adaptive Optics and spechles*

Since the 1990 adaptive optics (AO) are used. These change shape to undo the phase change of the atmosphere. However as these effects are unpredictable they always lack behind slightly. Further more they have errors them self, the phase is never completely corrected. Both these effects cause small distortions in the final image, these are known as spechles. Thus even with AO the total PSF for the atmosphere, the AO and the instrument will keep changing in time, however the magnitude of the change is severely reduced. Adaptive optics don not correct the entire field, generally each system has a control radius in which the AO can reduce the seeing.

-

2.2 VECTOR APODIZING PHASE PLATE

As mentioned in the introduction the vector apodizing phase plate is not a normal chronograph. The apodizing phase plate (APP) is a chronograph that changes amplitude of phase in the pupil plane to create destructive interference in an area of the PSF. This creates a dark zone on the PSF. Dim object imaged there can be resolved if the contrast between them and the star is smaller then the contrast between center peak of the PSF and the dark zone. Because the chronograph works in the pupil plane it is insensitive to the effects of spechles, further more unresolved stars do not limit how close to a star the chronograph can function.

The APP does this by introduces differences in the optical path length thereby changing the phase. These changes are designed to create the mentioned dark zone in the shape of a 180° half circle with a radius of 2 to 9 λ/D [1]. To do so optical the path length differences need to be different throughout the pupil, the design can be seen as

a heightmap of path differences. The APP is manufactured by directly printing that heightmap using liquid-crystal technology.

The vector apodizing phase plate (vAPP) is an upgrade to the APP that applies the path length differently mirrored to right and left handedly polerised light. By then splitting the right and left handed light and imaging both seperated we get not 180° of dark zone but 360° solving one of the major problems of the APP at a cost of brightness. However there is ample enough light that this is a small price to pay.

2.3 DISKS

With the formation of a star it is inevitable a disk will form due to to the conservation of angular momentum. While initially material will orbit in various directions and planes these will slowly cancel out due to collisions and attraction leaving the average plane and direction as the final orientation of a disk around the star. It seems likely these disk will allow the formation of planets due to the high detection rate of exoplanets [11].

The formation of discs goes through 3 main stages[11] :

1. Right after the molecular core collapses, most mass is still in a cloud surrounding the disk and the star. Due to that it is not possible to see the disk in the near-IR or optical regime.

2. Most mass moves into the star, the disk is obstructed by outflow of mass. The enveloping mass is about the same as the disks.

3. Central star becomes visible, the enveloping dust has cleared and the disk only contains a few percent of the total mass. It now is a protoplanetary disk.

During the first two stages the star is still forming, the disk is obstructed by dust and they take a relatively short time. However at the third stage we should be able to study the disk. After this stage planets can form, their formation process is uncertain.

It is suspected the disks features are linked to the formation of planets. Rings in a disk could indicate a planet embedded in the disk [6] however those planets can currently not be detected. There is also evidence that spirals in disks can be caused by planets in the disk [2]. This means the morphology of disks can provide valuable insight in how planets form.

2.3.1 *Categorization and features*

Disks seem to be ring or spiral shaped with some forms in between. They can be classified into 6 categories [2] see Figure 4.

Figure 4: Sketch summarizing the different classifications of protoplanetary disks proposed in [2]

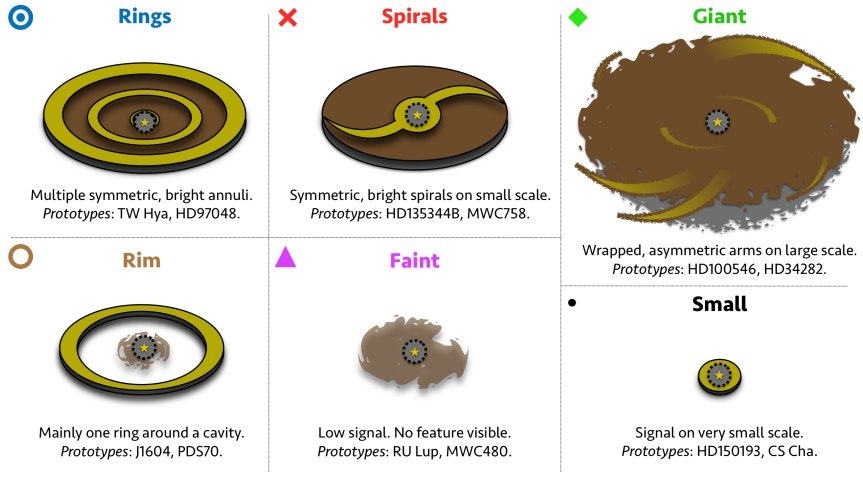

With this categorization they [2] further conclude:

- faint disks are young
- spiral disks are around stars that almost start their main sequence
- ring disk have no outer stellar companion

Furthermore they [2] conclude that in small disks of 10 to 20 Au in size and young faint disks structures remain undetected.

2.3.2 *Expected Contrast*

To get an upper limit on the brightness of a disk we assume all star light that hits the disk is reflected towards us. The light from a star drops quadratically as it gets farther away. Thus we will never have a disk brightness exceeding $1/R^2$. A disk at 1 AU from an run like star will have a brightness 2.1×10^{-5} of the star. At 5 AU this drops to 8.6×10^{-7}. This is the minimal contrast we can expect, as the density of the disk might make it less the optically thick.

2.4 ANGULAR DIFFERENTIAL IMAGING

angular differential imaging (ADI) is a technique to remove stationary and slowly changing PSF structures from an exposure. It is a proven method for the detection of companions with classic PSFs such as the one in Figure 2b.

The basis of ADI is to let the field of view rotate with respect to the coronograph and sensor during an observation. By then taking multiple short exposures anything off center will be rotated a bit in each

exposure. If the mean of all other exposures is subtracted from an exposure we lose most of the stars PSF. Once done for every exposure, rotating all the results so the field of view is aligned the median can be taken which gives the final image.

To use ADI with the vAPP we need to make sure the entire sequence fits in the dark hole.

3 DATA GENERATION

We choose not to use on sky data but create our own. This presents a number of advantages though the main reason is the lack of disk observations using the vAPP. Generating the data from a model allows us to vary paramaters as we wish. We can try a reduction method on a simple slightly inclined disk or a near face on disk with many rings. By reducing images of morpholocally differing disks we can map out how well a reduction method works for each morphology. Most importantly we can clearly separate artifacts created during data reduction from disk features when we know what the disk looks like.

3.1 DISK MODEL

We use a 2-dimensional disk model based on the work by [3]. The model has 4 basic parameters:

INCLINATION The angle the disk is tilted towards the observer. A 0 degrees inclination gives a face on disk and 90 degrees a horizontal line being an edge on disk. As illustrated in Figure 5b

POSITION ANGLE After inclination the disk can be rotated around the line of sight from the observer, rotation to the left is positive. See Figure 5a

INNER AND OUTER RADIUS Many disks start and stop at some radius from star. The inner and outer radius are relative to the field size that defaults to 10. An Inner radius of 2 gives a hole in the disk with a diameter 20% of the image width.

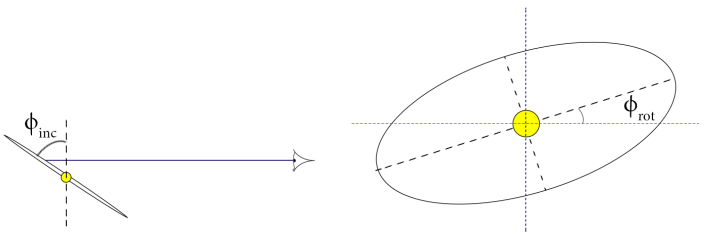

(a) Inclination angle from: [3] (b) Position angle, from: [3]

The disk is modeled as optically thick and does not emit light on its own. At a certain radii between the inner and outer radii the disks brightness is given by:

$$B(r) = B_{star} \cdot \left(\frac{r}{R_{star}}\right)^2 \tag{5}$$

We evaluate the model onto an image of 200 by 200 pixels. This not only speeds up our calculations it is around the expected resolution of an observed dataset. The model behaves well for most disks however on this resolution features that are small in the observers plane are pixilated as we see in Figure 6 below. This poses no problem as we do not expect to resolve such features.

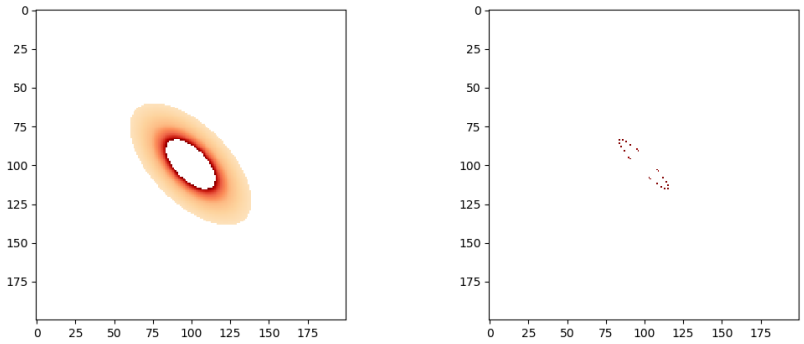

(a) model output for an inclination of 60 deg, an inner radius of 2 and an outer radius of 5

(b) model output for an inclination of 80 deg, an inner radius of 2.2 and an outer radius of 2.3

Figure 6: two disks created by the model with different size and inclination both with a position angle of 45 degrees

3.2 ATMOSPHERIC DISTORTIONS

To simulate an observation we do not use a single given psf. Since during an observation the combined psf of the atmosphere and instrument changes. However a complete simulation of these effects is outside the scope of the thesis. Instead try and approach a similar morphology to a on sky psf, with similar changes in time.

3.2.1 *Fourier method*

First we tried modifying a give single vAPP psf to get a set of disturbed psfs. To achieve this a pattern is added to the foerier transform of the psf before transforming it back from foerier space, see the equation below. The pattern is then shifted for every timestap.

$$\mathscr{F}_{2d}^{-1}\left(\text{intensity}\cdot\mathscr{F}_{2d}(\text{psf})\cdot\text{pattern}+(1-\text{intensity})\cdot\mathscr{F}_{2d}(\text{psf})\right) \tag{6}$$

The best results where achieved using a grid of blurred circles as pattern, see Figure 7. Note the distortions to the psf are clusterd

around the center of its peaks but not randomly spread. Clearly this will not do.

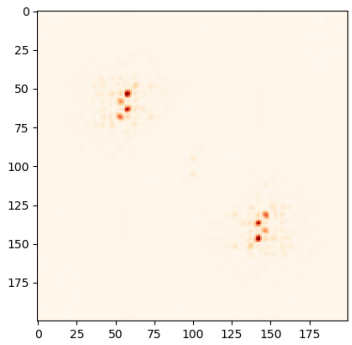

(a) difference between two psfs created using this method, the pattern has shifted 10 pixels

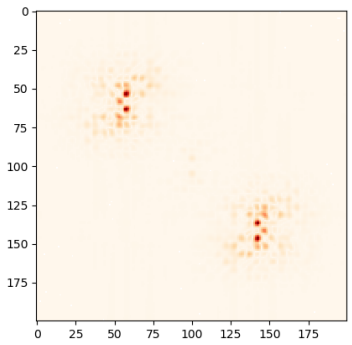

(b) difference between two psfs created using this method, the pattern has shifted 5 pixels

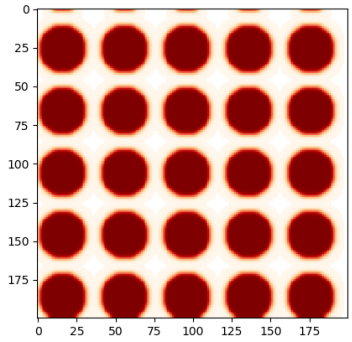

(c) pattern that is shifted and applied to the foerier space of a psf

Figure 7: Pattern (a) and the diffrences between psfs **distorted** with this pattern using the method described above

3.2.2 *Using HCIPy*

Then we tried a simulation of the psfs using high-contrast imaging python (HCIPy), an open-source object-oriented framework written in Python for performing end-to-end simulations of high-contrast imaging instruments [10]. The framework is used to generate PSFs with a very rough simulation. We use the provided methods in HCIPy to create a multi-layer atmospheric model that changes in time. Then we use that model, the vAPP amplitude and vAPP phase screen to generate a series of psfs. Instead of modelling an active optics system we modified the fried parameter for the atmosphere to get similar morphological changes in time to the availible on sky images. This is sufficient as the disk will always lie within the control radius of the

AO which means the effect of an AO system on the disk will mostly be a increase in resolution by reducing the seeing effect.

We use a telescope diamater of 8.2m and a wavelength, of $1 \cdot 10^{-6}$m for the generation. For a fried paramater of 4m we find quantativly similar psf morphologies to the on sky data. To put this into perspective: to simulate excellent seeing conditions we would use 20cm. With these setting we use HCIPy to create an orderd set of psfs changing through time as the simulated atmosphere evolves. See Figure 9 for the diffrence between the first psf in a set and later psfs in the same set. Note that as time evolves the differences grow.

3.3 GENERATING AN OBSERVATION

To get a dataset that simulates an obeservation we create an orderd set of disk images each one rotated a bit to eachother. This accounts for the field rotation between exposures caused by observing with an alt azimuth telescope. The angle depends on the time between exposures and the field rotation rate.

$$\psi = 0.2506 \cdot \frac{\cos(A)\cos\phi}{\sin(z)} \tag{7}$$

The field rotation ψ in degrees per minute for a given target azimuth A, zenith distance z and telescope latitude ψ [8, page 95]. If we would be observing from mauna kea (latitude 19.8) at a resonable 30 degrees from the zenith this gives a rotation rate between 0 and 14.74 degrees per minute.

Now to get the simulated observation an orderd set is created by convolving each n-th image from the disk set with the n-th image of the psf set. These are the simulated observations through time.

Using variations on this method we create 3 different sets.

1. Place the star as a single pixel with value one in the center of the disk before going through the above procedure. This is our observation set.

2. Leave out the disk, place only the single pixel in the center representing the star. This can be useful for checking if data reduction algoritmes work properly.

3. Leave out the star, this way we see what the vAPP does to the extended disk.

For each of the sets we can generate an additional variant to look at what the best result attainable is by leaving out the psf distortions. We do this by taking the convolution of the n-th disk image with the first PSF of the PSF set instead of the n-th.

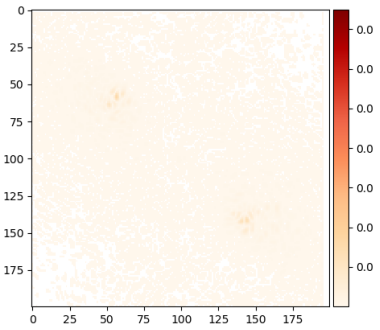

(a) simulated psf: 1e - 2e, 0.7 seconds difference

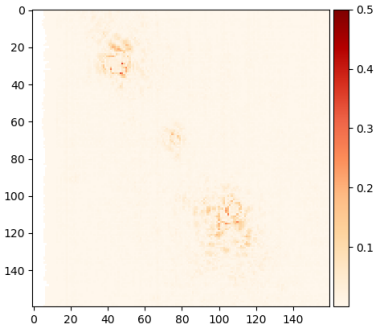

(b) on sky psf: 1th - 2th, *** seconds difference

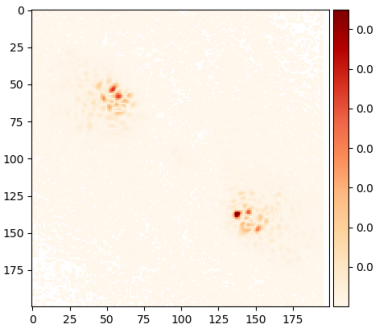

(c) simulated psf: 1th - 10th, 7 seconds difference

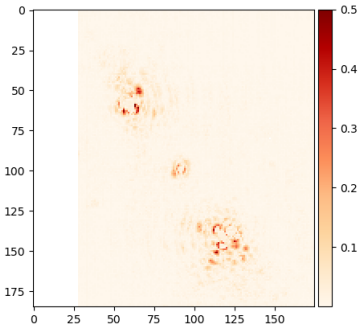

(d) on sky psf: 1th - 10th, *** seconds difference

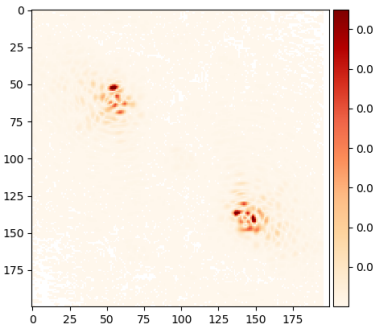

(e) simulated psf: 1th - 50th, 14 seconds difference

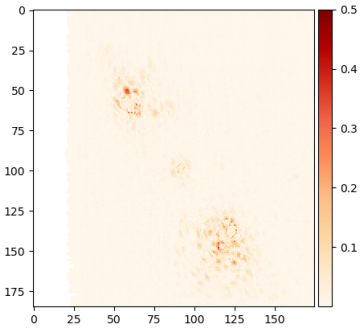

(f) on sky psf: 1th - 50th, *** seconds difference

Figure 8: Differences between the first psf of an observation and later psfs. Compared between simulated observations on the left and on sky data on the right. The psfs where aligned then normalised on the maximum of the leakage term, finally the absolute value of the diffrence between the first and n-th psf was taken. The second, 10th and 50th simulated psf are 0.7, 7 and 14 seconds apart in the simulation

4 DATA REDUCTION

The generated exposures contain 2 mirrored dark zones and are shifted relative to eachoter by the changing PSFs, see **??**. Before applying any post processing technique we create 2 aligned stacks of processed exposures. Then we apply the ADI algoritme to remove most of the star light.

4.1 PRE-PROCESSING

Before we extract the **psf kernals** we align the exposures. We find the shift relative to the vAPP instrument PSF for every exposure in the set by cross correlating the upsampled image. Then the images are shifted using spline interpolation[1]. For the implementation of both algoritmes we use the SciPy libarary[5].

To find the center of the **psf kernals** an exposure is devided left right. Now for each half the brightest pixel gives the center, around it we copy out a square with sides of 30% of the image width. Done for all exposures this gives the 2 aligned stacks, a slice of which we see in Figure 9b and Figure 9c.

4.2 ANGULAR DIFFERENTIAL IMAGING

4.2.1 *Algoritme*

Now there are two seperate stacks of exposures we apply the ADI algoritme [7] to each. First the median is taken over the stack using the implemantion provided by the numby libarary [9]. This is our reference PSF. After subtracting the reference PSF from each exposure we rotated it back so the fields of all exposures are aligned again (see Section 3.3). Rotating a square inside a containing square here we lose information as the right angles rotate out of the containing square. The empty space that appears at the containing squares right angles is filled with value 0. The pixel values are determined by spline interpolating. For the rotation algortime we use again the SciPy libarary [5].

Finally we take the median over the processed exposures to get a the end result.

1 Here an image is interpolated by fitting multiple polynomials called splines

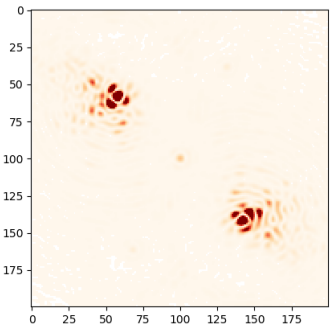

(a) Exposure after aligment

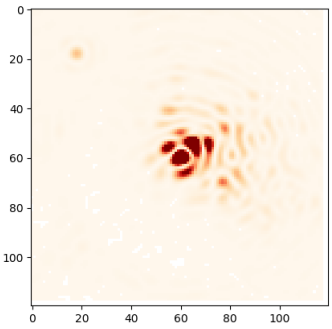

(b) left **psf kernal**

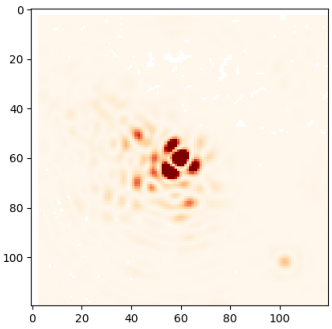

(c) right **psf kernal**

Figure 9: A generated exposure through the Pre-processing process, first it is aligned and then its right and left **psf kernal** are extracted

4.2.2 *Control*

Now we check if the algortime works applying it to an exposure set with only the star and no distortions applied. This results in a completely black image as expected. Next we apply ADI to an exposure set with only the star and distortions applied, this results in a circular noise pattern on the left and right as seen in Figure 10).

4.3 PAREMATER STUDY

When observing disks we are most intersested in theire morphology. It could however be heavily affected by the vAPP and ADI. As the vAPP by design redestributes licht in an uneven way and ADI removes rotational symmetry while disks are by nature quit rotationally symmetrical. To see how the output morphology resembles the that of the input model we generate exposure stacks for a number of disks with different paramaters. We vary the number of rings, the width of the rings and the inclination. We keep the contrast between the disk and star unrealisticly low. For the best results of the paramater study the

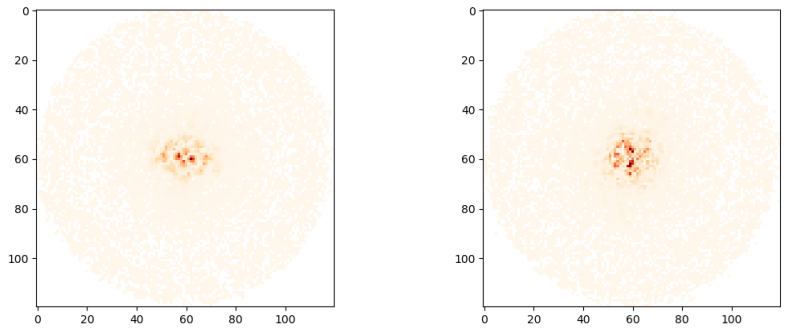

(a) Left region after ADI

(b) right region after ADI

Figure 10: The right and left end result of ADI applied to a generated exposure stack of a star. The stack contains 20 exposures, the field rotation over the entire stack is 60°. Note how derotating the fields leads to a circular result as we lose the angles.

contrast is then returned to a realistic value. This allows us to easily compare results.

For each model the following images are generated:

I An exposure of the model with a central star, using a distorted PSF.

II The result of ADI for the model with a central star using distorted PSFs.

III An exposure of the model without a central star, using the undistorted PSF.

IV The result of ADI for the model without a central star using the undistorted PSF.

These images help see how the model behaves as we could observe it (I and II) and how only model is imaged when we remove anything that would distort or distract from it (III and IV). The latter is done by removing the star and using a fixed PSF. Using III and IV we can determine weather using the vAPP and ADI could give usable results. We expect the morphology of the post processed disks to differ from the models input. However we expect the the new morphology to be unique for the input model or some of its paramaters.

5

RESULTS

Disk	Number of rings	Width of rings	Inclination
Gnat	per gram	13.65	80
Gnu	stuffed	92.50	70
Emu	stuffed	33.33	60
Armadillo	frozen	8.99	70

6 DISCUSSION

Instead of taking the mean of all other exposures as reference PSF another approch to use a few images close in time as possible as reference sequence [7]. As there is less time between the exposures the PSF has changed less due to seeing (see: Section 2.1.2) giving a greater correlation between the features on the reference image and the individual image. The disadvantage is that pixel to pixel noise is rejected less as we now only take an median over a slightly rotated sample. Care must be taken that the reference sequence has enough field rotation to displace features of intrest by at least 1.5· PSF full width half maximum (FWHM). This ensures we don not subtract the feature from itself.

BIBLIOGRAPHY

[1] David S. Doelman, Frans Snik, Nathaniel Z. Warriner, and Michael J. Escuti. "Patterned liquid-crystal optics for broadband coronagraphy and wavefront sensing." In: *Proceedings SPIE 10400, Techniqes and Instrumentation for Detection of Exoplanets VIII* (2017).

[2] Antonio Garufi et al. "Evolution of protoplanetary disks from their taxonomy in scattered light: spirals, rings, cavities, and shadows." In: (Oct. 2018).

[3] Okko van der Haak and Pieter Speelman. "Stellar disk reconstruction using Spectro-polarimetry." Bachelor Thesis. June 2018.

[4] Eugene Hecht. *Optics. International Edition*. Pearson, 2002.

[5] Eric Jones, Travis Oliphant, Pearu Peterson, et al. *SciPy: Open source scientific tools for Python*. [Online; accessed 21 may 2019]. 2001–. URL: http://www.scipy.org/.

[6] Giuseppe Lodato et al. "The newborn planet population emerging from ring-like structures in discs." In: *Monthly Notices of the Royal Astronomical Society* 486 (Mar. 2019), pp. 453–461.

[7] Christian Marois, David Lafreniere, Rene Doyon, Bruce Macintosh, and Daniel Nadeau. "Angular Differential Imaging: A Powerful High-Contrast Imaging Technique." In: *The Astrophysical Journal* 641.1 (2006), pp. 556–564. DOI: 10.1086/500401. URL: https://doi.org/10.1086%2F500401.

[8] Ian S. McLean. *Electronic Imaging in Astronomy*. Springer, 2008.

[9] Travis Oliphant. *NumPy: A guide to NumPy*. USA: Trelgol Publishing. [Online; accessed 22 may 2019]. 2006–. URL: http://www.numpy.org/.

[10] E. H. Por, S. Y. Haffert, V. M. Radhakrishnan, D. S. Doelman, M. Van Kooten, and S. P. Bos. "High Contrast Imaging for Python (HCIPy): an open-source adaptive optics and coronagraph simulator." In: *Adaptive Optics Systems VI*. Vol. 10703. Proc. SPIE. 2018. DOI: 10.1117/12.2314407. URL: https://doi.org/10.1117/12.2314407.

[11] Jonathan Williams and Lucas Cieza. "Protoplanetary Disks and Their Evolution." In: *Annual Review of Astronomy and Astrophysics - ANNU REV ASTRON ASTROPHYS* 49 (Mar. 2011). DOI: 10.1146/annurev-astro-081710-102548.